ELSEVIER

Journal of Magnetism and Magnetic Materials 174 (1997) 40–56

Journal of magnetism and magnetic materials

Interplay between structure and magnetism in Fe/Cu(1 0 0) upon temperature variation

M. Zharnikov*, A. Dittschar, W. Kuch, C.M. Schneider, J. Kirschner

Max-Planck-Institut für Mikrostrukturphysik, Am Weinberg 2, D-06120 Halle/Saale, Germany

Received 3 February 1997

Abstract

Interleaved low-energy electron diffraction (LEED) and magneto-optical Kerr effect (MOKE) measurements were carried out for room-temperature epitaxially grown FCC-like Fe/Cu(1 0 0) in the temperature range of 120–400 K. The structure of the Fe film was found to be not only dependent on thickness, as was believed previously, but also to be influenced by the temperature. Temperature-driven structural transitions were observed in the 4 and 4.5 ML films, this effect being more pronounced at 4 ML thickness. Whereas the whole 4 ML film assumes an FCC-like structure with a strong tetragonal expansion (FCT-like) at temperatures below 313 K, the bulk of the film relaxes into the 'isotropic' FCC-like structure and only the top layers remain expanded at temperatures above 333 K. Because only the FCT-like (expanded) Fe possesses ferromagnetic properties, the film becomes paramagnetic after heating above 333 K. This finding represents a new type of magnetic order–disorder transition and explains the lower value of the Curie temperature in the 4 ML Fe film as compared to 3 ML. In the 4.5 ML Fe film the similar correlation between the temperature-driven structural transition and an occurrence of the ferromagnetic long-range order was observed. Additionally, a pronounced difference in the energy positions of the characteristic maxima in the LEED $I(E)$ curves for the (0 0) beam as well as a kinematic analysis of these curves imply a difference in the value of the tetragonal expansion for the entirely expanded FCC-like Fe film and the film expanded only in the topmost layers.

Keywords: Structure; Thin films; Order–disorder transition

1. Introduction

The relationship between structural and magnetic properties has since long been a fascinating field of studies in solid state physics. One of the most famous examples of such a relationship is FCC-Fe where total magnetic moment calculations predict ferromagnetic ground states at an increased atomic volume, otherwise antiferromagnetic ordering is expected [1, 2]. This prediction can be verified only in ultrathin films of iron epitaxially grown on FCC surfaces, because FCC-Fe represents a metastable phase and exists as bulk material only above 1184 K. As a suitable substrate, Cu(1 0 0) has

* Corresponding author. Present address: Angewandte Physikalische Chemie, Universität Heidelberg, Im Neuenheimer Feld 253, D-69120, Heidelberg, Germany. Tel.: + 49 6221 544921; fax: + 49 6221 546199.

PII S0304-8853(97)00220-5

been chosen in most of the experimental studies, because of its diamagnetic properties as well as a small positive misfit of $\approx$1–2% with respect to FCC-Fe (the lattice constants of Cu and FCC-Fe at room temperature are 3.61 Å and 3.55–3.58 Å, respectively [3]) forcing an increased lattice spacing in the pseudomorphic Fe film. The structural phase diagram of Fe/Cu(1 0 0) was found to be rather complicated; the structure of the film depends both on the growth conditions (mainly the substrate temperature) and thickness [3–11]. For room-temperature-grown films an FCC-like structure exists only at thicknesses d below 11–12 monolayers (ML) (if no surfactants are used [12, 13]); at higher d an FCC–BCC structural phase transformation occurs [14–16] which is accompanied by a switching of the easy axis of the magnetization from perpendicular direction ($d < 11$–12 ML) to in-plane [17–20].

The expected enlargement of the lattice spacing in FCC-like Fe on Cu(1 0 0) takes place both in lateral (pseudomorphic growth) and vertical directions, the vertical interlayer spacing $a_\perp$ being mainly affected. This expansion occurs, however, not at all thicknesses where the FCC-like phase exists. Detailed low-energy electron diffraction (LEED) investigations [3, 5–8] using the tensor LEED technique [21] to fit experimental $I(E)$ curves showed that only for $d \leqslant 4$ ML the entire room-temperature-grown Fe film assumes a tetragonally expanded FCC structure (FCT) with an enlarged atomic volume $V_a \approx 12.1$ Å^3 ($a_\perp \approx 1.87$ Å); this structure is characterized by pronounced (and coverage-dependent) vertical buckling (up to 0.2 Å) and lateral shifts and can only on the average be considered as a FCT one. At higher thicknesses only the two topmost layers keep a larger value of $a_\perp$, whereas the bulk of the film relaxes into the 'isotropic' (also on the average) FCC-like structure ($a_\perp \approx 1.78$ Å, $V_a \approx 11.4$ Å^3). The value of the remanent magnetization M_R in FCC-like Fe/Cu(1 0 0) is observed to correlate with this structural behavior: an almost linear increase of the magnetization takes place up to $d \approx 4$ ML, whereas M_R drops down at higher thicknesses and remains approximately constant between 5 and 10 ML [17, 18]. Such a behavior of the remanent magnetization can be easily understood if one assumes that the ferromagnetism in the film is directly related to the enlarged atomic volume (expanded interlayer distance). This assumption was recently substantiated by nonlinear magneto-optical Kerr effect (MOKE) measurements [22] and by conversion-electron Mössbauer spectroscopy experiments [23–25]. These experiments also showed that 'isotropic' FCC-like Fe in fact orders antiferromagnetically, in agreement with the results of a previous magneto-optical Kerr effect investigation [18]. There remains some uncertainty in the value of the corresponding Néel temperature, because the values provided by the Mössbauer spectroscopy experiments ($\approx$70 K) and extrapolated Kerr effect measurements ($\approx$200 K) are rather different.

Thus, structural and magnetic properties of room-temperature-grown Fe/Cu(1 0 0) closely correlate with each other as function of thickness and are believed to be well understood. One should consider, however, that both the magnetic measurements and LEED investigations were carried out at relatively low temperature ($\approx$90 K). The structure of the films which seems to have the crucial influence on their magnetic properties was assumed to depend only on thickness and remain unaffected by other parameters, in particular, by the temperature (only some indirect indications of the temperature-driven structural transformation in the Fe/Cu(1 0 0) grown at 100 K were observed previously [26, 27]). The questions whether the structure of these films at a fixed thickness remains stable against temperature variation and whether possible temperature-driven structural transformations are accompanied by a change of magnetic properties were open until our recent short publication on this subject [28]. In this paper we will address both these questions in more detail and present the results on the temperature dependence of the structural and magnetic properties of FCC-like Fe/Cu(1 0 0) in the temperature range of 120–400 K. As compared to our previous report [28] the data for all thicknesses will be presented and analyzed, thus, providing a more complete and consistent picture.

2. Experimental procedure

The experiments were performed in a UHV chamber [29] equipped with facilities for Auger

electron spectroscopy (AES), LEED, MOKE, medium-energy electron diffraction (MEED) and thin film growth; a schematic drawing of the chamber is presented in Fig. 1. The base pressure was 1×10^{-8} Pa.

The iron films with thicknesses of 2–12 ML were epitaxially deposited on a Cu(1 0 0) single crystal held at room temperature. The deposition rate was varied between 0.3 and 0.6 ML/min and the pressure during the evaporation was below 2×10^{-8} Pa. The growth process was monitored and controlled in situ by MEED, with the typical curve for the specular beam (Fig. 2) being reproduced in our experiments [17]. This procedure and additional AES measurements allowed a thickness determination with an accuracy of 0.2 ML. No surface contaminations above the AES detection limit ($\approx 1\%$) were found after iron deposition.

The magnetic properties were probed using the MOKE facility by registering the hysteresis loops in the polar geometry. The corresponding setup (see Fig. 1) included a stabilized HeNe laser ($\lambda = 633$ nm), a photoelastic modulator, a polarization filter and an integrated photodiode/amplifier. The signal was detected by using a lock-in technique; for this purpose the incident laser beam was sinusoidally modulated between left and right circular polarization. The hysteresis loops had

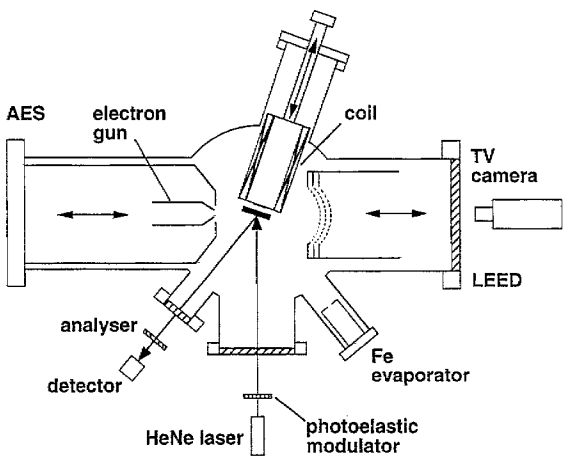

Fig. 1. Schematic drawing of the experimental setup. The sample is in the position for the MOKE measurements.

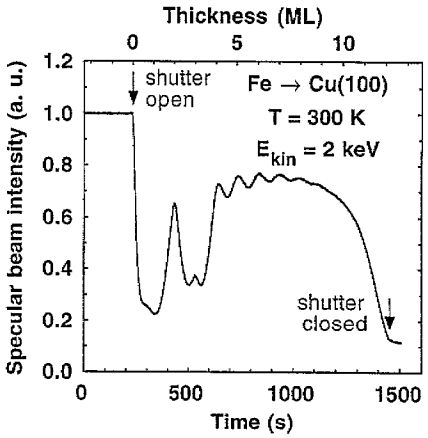

Fig. 2. Intensity of the MEED specular beam during room temperature growth of 12 ML Fe film on Cu(1 0 0). The intensity at reflection from clean Cu(1 0 0) is normalized to one. The primary beam was directed along the [0 0 1] azimuth of the substrate with polar angle of incidence of 3–5°.

a square shape except for the region near the Curie transition where a pronounced change of the shape of the loops, namely, a strong reduction of the remanence as compared with the saturation magnetization was observed; in other words, the loops became inclined. The maximum magnetic field applied H_{max} was 250 Oe which allowed us to reach the saturation magnetization over most of the temperatures and thicknesses investigated (for 4.5 ML $\leqslant d \leqslant$ 10 ML the coercivity at temperatures below 190–210 K exceeded H_{max} – this region has no relevance to the main subject of this article). The magnetic properties of BCC Fe/Cu(1 0 0) ($d >$ 10 ML, in-plane magnetization) were not measured.

Conclusions on the crystalline structure of the films were mainly drawn from a kinematic analysis of LEED $I(E)$ curves for the (0 0) diffraction beam. These curves often show a group of periodic (as a function of $\sqrt{E}$) intensity maxima that result from constructive interference whenever the vertical interlayer spacing corresponds to an integer multiple of the electron wavelength [30, 31]. Such a group of maxima thus, represents a kind of fingerprint for a definite structural phase in the system under investigation. The main advantage of the $I(E)$

curves for the (0 0) beam is the extremely short time needed for their acquisition and analysis which allows direct monitoring of structural transformations in the system investigated. Moreover, it is possible to evaluate (in the kinematic approximation) the corresponding average vertical interlayer spacing, being especially beneficial in a system where the magnetic properties are determined predominately by this parameter.

Of course, the analysis of a single $I(E)$ curve is not intended to compete with the tensor LEED fitting procedure involving a couple of different $I(E)$ curves relating to the details of the investigated structure (superstructure, buckling, etc.). Such a procedure needs, however, an enormous expenditure of time if one considers the whole data set to be measured and processed when both the film thickness and temperature are varied. The details are of importance to understand the dynamics of the structural transformation in Fe/Cu(1 0 0), but play a secondary role in the magnetic properties of this system.

It should also be noted that the kinematic analysis represents, strictly speaking, rather a qualitative than a quantitative method because this approximation ignores the real character of the electron–atom scattering as well as multiple-scattering events. Nevertheless, the kinematic approach seems to work for thin films of 3d-metals: this approach was successfully used to investigate the structure of $Fe/Cu_3Au(1\,0\,0)$ [32] as well as epitaxial FeCo alloys on Cu(1 0 0) [33] and Ni/Cu(1 0 0) [34]; the kinematic analysis was also previously applied in the case of Fe/Cu(1 0 0) to study the structure of the surfactant-stabilized FCC-like Fe [13]. Anyway, a large set of experimental data ($I(E)$ curves for the (0 0) beam) and comparison of at least some results of the kinematic analysis with the output of the dynamical LEED calculations is necessary for the correct interpretation of the experimental $I(E)$ curves and for the judgement whether the kinematic approximation is applicable in the case under consideration.

The LEED $I(E)$ curves for the (0 0) diffraction beam were taken at an angle of incidence of 6° in the (0 0 1) mirror plane of the substrate; a special computer-controlled video-LEED system based on a Macintosh computer was used [35] (this system was also used for the MEED measurements). Some LEED patterns were also taken to look for the superstructures previously observed in the LEED investigations [3, 5–8]. The patterns were measured only at low temperatures (≈ 150 K); the samples were usually cooled down to ≈ 150 K directly after the evaporation because we wanted to start at conditions typical for the foregoing studies. After this initial cooling, the measurements of structural and magnetic properties at variation of the temperature were carried out, the latter being varied in steps of 5–30 K depending on the observed temperature behavior of the hysteresis loops and $I(E)$ curves.

At some fixed thicknesses these measurements were carried out in an interleaved mode to exclude irreversibility effects. For this purpose, the sample was rapidly rotated between the MOKE and LEED facilities at each fixed temperature. After these measurements the temperature was changed and the whole procedure was repeated until the temperature scan was completed. It took about 10–15 min to make both the MOKE and $I(E)$ measurements at a fixed temperature and approximately 5–15 min to change the temperature, depending on the temperature step.

To exclude the influence of interdiffusion, the maximum temperature Fe/Cu(1 0 0) may be heated to had to be noticeably less than that for the onset of interdiffusion (410 K [15, 36], 340–400 K [37]). At the same time, we were interested to follow the structure of the film through the magnetic order–disorder transition. The region of this transition is especially interesting from the point of view of the possible temperature-driven structural transformation concerning a link between magnetism and structure in Fe/Cu(1 0 0). Therefore, the maximum temperature for all thicknesses except for 2 and 3 ML was limited to about 350 K. For 2 and 3 ML this value was about 363 and 393 K, respectively, because of the high values of the Curie temperature for these thicknesses [17, 18].

3. Results

In this section the results are presented in three separate parts: (1) structure of Fe/Cu(1 0 0) as

a function of thickness, (2) structure of Fe/Cu(1 0 0) as a function of temperature and (3) magnetic properties of Fe/Cu(1 0 0) as a function of thickness and temperature. The discussion of the results is given in Section 4.

3.1. Structure of Fe/Cu(1 0 0) as a function of thickness

In Fig. 3a, $I(E)$ curves for the (0 0) LEED beam for clean Cu(1 0 0) and Fe/Cu(1 0 0) at various thicknesses d are depicted; the corresponding values of $a_\perp$ calculated from these curves within the kinematic approximation are presented in Fig. 4a. The $I(E)$ curves in Fig. 3a were collected at $T = 153$ K (except for clean Cu) which, on the one hand, lies significantly below the Curie temperature of the films [17], and, on the other hand, are typical for previous LEED measurements on Fe/Cu(1 0 0) [3, 5–9]. Thus, a direct comparison of our data with the tensor LEED results can be made. This should be a crucial check whether the kinematic approximation can be successfully used in the present case of Fe/Cu(1 0 0).

The $I(E)$ curve for clean Cu(1 0 0) in Fig. 3a reveals a group of maxima (marked by the dotted lines) which can be identified as the kinematic ones; the energy positions E_n of these maxima are depicted in Fig. 5a as a function of n^2, where n is an integer number. Generally, the energy positions of

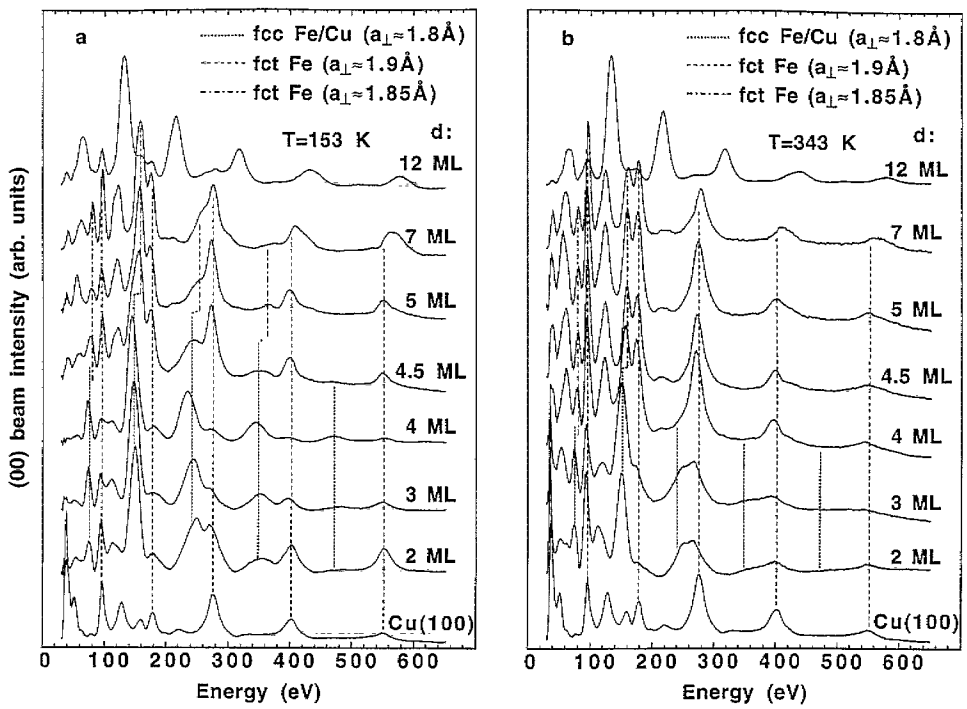

Fig. 3. Intensity vs. energy dependence of the LEED (0 0) beam from Fe/Cu(1 0 0) measured at temperatures 153 K (a) and 343 K (b); the $I(E)$ curves for 2 and 3 ML Fe films in (b) were measured at 363 and 393 K, respectively. The kinematic maxima related to the FCC-like and two different FCT-like structures of Fe on Cu(1 0 0) are traced by vertical dashed, dotted and dashed-dotted lines, respectively. The dashed lines are also used to trace the analogous maxima for Cu(1 0 0). The energy positions of these maxima and the $I(E)$ peaks related to the FCC-like Fe practically coincide because of the same value of $a_\perp$ for Cu(1 0 0) and FCC-Fe. A change of the tetragonal distortion in FCT-like Fe with increasing coverage can be directly seen as a shift of the corresponding kinematic maxima between 4 and 5 ML in (a) and between 3 and 4 ML in (b).

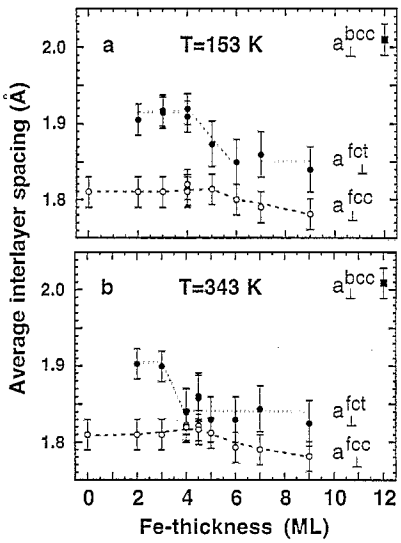

Fig. 4. Thickness dependence of the vertical interlayer distances $a_\perp$ for the FCC-like and FCT-like Fe on Cu(1 0 0) (open and full circles, respectively) at temperatures 153 K (a) and 343 K (b). The full square represents $a_\perp$ for the BCC-like Fe/Cu(1 0 0). The values of $a_\perp$ in (a) and (b) were calculated within the kinematic approximation from the $I(E)$ curves in Fig. 3a and Fig. 3b, respectively. The dotted (FCT-like Fe) and dashed (FCC-like Fe) lines represent a guide to the eye. At small thicknesses ($d \leqslant 4$ ML) the full circles represent the value of $a_\perp$ for the clean Cu(1 0 0) rather than for the FCC-like Fe; anyway these values are approximately the same. The $I(E)$ peaks related to the FCC-like Fe and Cu(1 0 0) practically coincide, the latter contribution being damped with increasing thickness of the Fe overlayer.

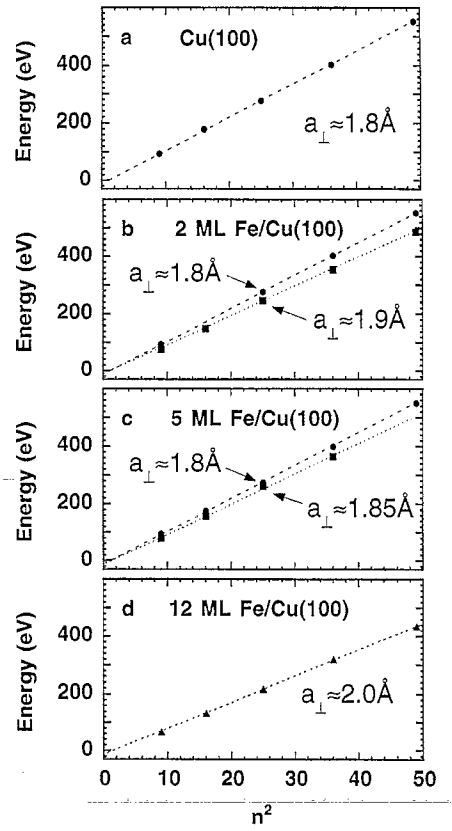

Fig. 5. Energy positions of the 'kinematic' $I(E)$ maxima vs. the index n^2 for Cu(1 0 0) (a), 2 ML Fe/Cu(1 0 0) (b), 5 ML Fe/Cu(1 0 0) (c), and 12 ML Fe/Cu(1 0 0) (d): the values of $a_\perp$ were obtained from the slope of the straight lines. The corresponding $I(E)$ curves are depicted in Fig. 3a. The maxima relating to the FCC-Cu/FCC-like Fe, FCT-like Fe (two different values of $a_\perp$) and BCC-like Fe are presented by the full circles, full squares and full triangles, respectively. The straight lines represent linear fits to the dependences $E_n(n^2)$. A linear dependence of E_n on n^2 indicates the kinematic origin of the intensity maxima.

the intensity maxima within the kinematic scattering treatment are given by the Bragg condition $a_\perp = n\lambda$ (for the normal incidence) which can be rewritten in the form

$$E_n = \frac{\hbar^2}{2m}\left(n\frac{2\pi}{a_\perp}\right)^2 + V_0,$$

where V_0 is the inner potential. The dependence $E_n(n^2)$ represents thus a linear function, the value of $a_\perp$ being derived from its slope. As it is clearly seen in Fig. 5a, such a linear dependence is, in fact, observed in the case of Cu(1 0 0), indicating the kinematic origin of the intensity maxima marked in Fig. 3a. The corresponding value of $a_\perp$ (corrected for the incidence angle) in Fig. 4a correlates rather well with the interlayer spacing in a Cu single crystal along the [1 0 0] axis.

The deposition of 2 ML Fe onto Cu(1 0 0) results in the appearance of an additional group of kinematic intensity maxima (marked by the dotted lines in Fig. 3a); the energy positions of the maxima are depicted by the full squares in Fig. 5b. Both the pronounced downward shift in the energy positions

of these maxima as compared to those for Cu(1 0 0), as well as the corresponding value of $a_\perp$ (Fig. 4a) allow us to associate these maxima with the tetragonally expanded FCC lattice of Fe (FCT-like Fe). With increasing d up to 4 ML the relative intensity of the maxima related to the FCT-like Fe increases, whereas the relative intensity of the $I(E)$ peaks associated with Cu becomes smaller. This behavior obviously stems from the attenuation of the Cu contribution by the Fe overlayer with the FCT-like structure.

An increase of d by only 0.5 ML from 4.0 to 4.5 ML changes the character of the $I(E)$ curves dramatically. A new group of the kinematic maxima with energy positions (depicted by the full circles in Fig. 5c) practically coinciding with the positions of the $I(E)$ peaks related to Cu, develops and becomes dominating at higher energies, whereas the maxima associated with FCT-like Fe shift a little upwards in energy (corresponding energy positions are depicted by the full squares in Fig. 5c) and keep a pronounced intensity only at low energies. They may therefore be associated with low-energy electrons having a small escape length, which suggests that the tetragonal expansion in this case is retained only in the upper layers of the film. The lower intensities of these maxima as compared with those for the structure associated with the FCT-like Fe in the $I(E)$ curve for the 2 ML film implies a smaller quantity of the FCT-phase in the case under consideration; the tetragonal expansion therefore, seems to occur exclusively between topmost and topmost but one layers of the 4.5 ML film (except for some small quantity of FCT-like Fe which still remains in the inner layers).

As to the new group of the kinematic maxima, it cannot be associated with the strongly attenuated signal of Cu but only with the FCC-like Fe; considering that the latter has practically the same lattice constant as Cu. This results in the same structure as was concluded previously from detailed LEED investigations [3, 5, 6] for the thickness under consideration: the inner layers of the Fe film have FCC-like structure and only the topmost layers are tetragonally expanded. A large similarity of the $I(E)$ curves at 4.5 ML $\leqslant d \leqslant$ 10 ML implies that such a structure is characteristic for all films in this thickness range, in complete agreement with the previous results [3, 6]. Also in such an agreement the character of the $I(E)$ curves changes distinctly at $d >$ 10 ML, manifesting the FCC–BCC structural transition. The curve for a 12 ML Fe film in Fig. 3a reveals only one group of the kinematic maxima with the energy positions depicted in Fig. 5d. The strong downward shift of these maxima with respect to the $I(E)$ peaks related to the FCC-like and FCT-like Fe as well as the corresponding value of $a_\perp$ in Fig. 4a allow us to associate this group of the maxima with BCC-like Fe. Only some weak contributions from the FCC-like and FCT-like Fe remain visible and can be observed at low energies.

The shift of the maxima related to FCT-like Fe in 4.5 ML film as compared to the analogous maxima at lower thicknesses is much more pronounced at 4.5 ML $< d \leqslant$ 10 ML, therefore, we did not present the data for the 4.5 ML film but for the 5 ML film in Fig. 5c. The shifted sequence is marked by the dashed-dotted lines in Fig. 3a; corresponding values of $a_\perp$ in Fig. 4a are less by $\approx$ 0.05 Å than the analogous values at $d \leqslant$ 4 ML (1.9 Å). In the case of 4.5 ML the kinematic maxima associated with the FCT-like Fe represent a superposition of two groups of the kinematic $I(E)$ peaks which are related to the two different FCT-like structures of Fe (different tetragonal distortion).

3.2. Structure of Fe/Cu(1 0 0) as a function of temperature

Increasing the temperature does not result in a simple uniform reduction of the heights of the peaks in the $I(E)$ curves but affects the various structures in these curves to a different extent. Except for the case of 4 and 4.5 ML which are rather specific and will be presented separately, two main tendencies are observed. First, the relative weight of the maxima related to FCT-like Fe decreases with increasing temperature as compared to the respective $I(E)$ peaks associated with Cu ($d \leqslant$ 3 ML) and FCC-like Fe (5 ML $\leqslant d \leqslant$ 10 ML). Second, the $I(E)$ peaks at higher kinetic energies are attenuated stronger than the peaks at lower kinetic energies. This is especially pronounced in the case of the maxima related to FCT-like Fe. Because of the continuous character of these changes (except for

the case of 4 and 4.5 ML) we refrain from presentation of temperature dependences of the $I(E)$ curves for every thickness, but include in Fig. 3b only the curves measured at the highest temperature to illustrate such a development. The analysis of the observed tendencies in the temperature behavior of the $I(E)$ curves will be presented in Section 4; the energy dependence of the Debye–Waller factor and the specific properties of the surface atoms will be taken into account.

As was noted at the end of the previous subsection, two groups of the kinematic maxima relating to two inequivalent FCT-like structures of Fe (different tetragonal distortion) are simultaneously presented in the $I(E)$ curve for the 4.5 ML Fe film at $T = 153$ K. With increasing temperature the relative weights of these two groups change which can be clearly seen in Fig. 6 where the corresponding $I(E)$ curves at different temperatures during heating are depicted; the maxima in the groups are marked by the dotted ($a_\perp \approx 1.9$ Å) and dashed-dotted ($a_\perp \approx 1.85$ Å) lines. In the temperature range 293–313 K the $I(E)$ peaks related to the FCT-like structure with a larger tetragonal distortion ($a_\perp \approx 1.9$ Å) disappear completely and only the features stemming from the FCT-like structure with the smaller tetragonal distortion ($a_\perp \approx 1.85$ Å) remain. These features are observed only at low energies which suggests that the corresponding tetragonal distortion occurs exclusively in the topmost layers of the 4.5 ML Fe film.

The case of 4 ML film is even more interesting. As was mentioned before, the whole film is tetragonally expanded at low temperatures revealing itself in the $I(E)$ curve in Fig. 3a: the maxima related to the FCT-like Fe represent the main structure and only strongly damped $I(E)$ peaks from Cu are observed. Upon heating this curve changes dramatically, the most abrupt changes occurring between 313 and 333 K (see Fig. 7 where the corresponding $I(E)$ curves at different temperatures are depicted). On the one hand, the $I(E)$ peaks related to Cu and FCC-like Fe become dominant. On the other hand, the $I(E)$ peaks associated with the FCT-like Fe which were observed at lower temperatures ($a \approx 1.9$ Å) disappear completely, and a new group of maxima related to the FCT-like Fe with $a_\perp \approx 1.85$ Å appears. The maxima in this new

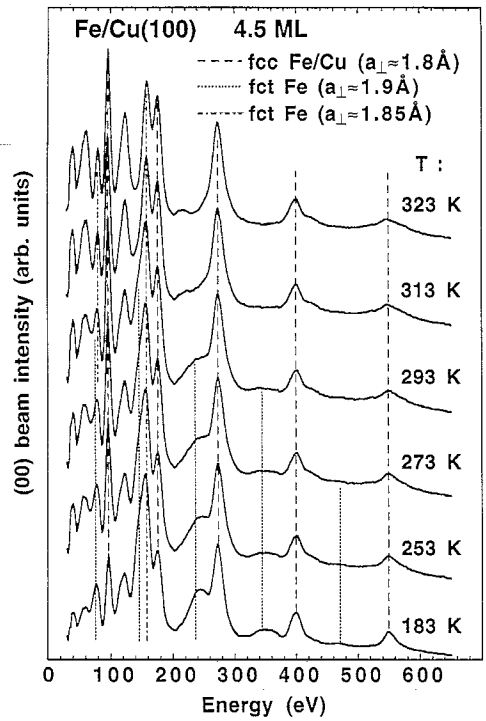

Fig. 6. Intensity versus energy dependence of the LEED (0 0) beam for 4.5 ML Fe on Cu(1 0 0) measured at various temperatures during heating. The kinematic maxima related to the FCC-like and two different FCT-like ($a_\perp \approx 1.9$ and 1.85 Å) structures of Fe on Cu(1 0 0) are traced by vertical dashed, dotted and dashed-dotted lines, respectively. In the temperature range 293–313 K the $I(E)$ peaks associated with the FCT-like structure with the larger tetragonal distortion ($a_\perp \approx 1.9$ Å) disappears completely and only the features stemming from the FCT-like phase with the smaller tetragonal distortion ($a_\perp \approx 1.85$ Å) remain. These features are then observed only at low energies.

group are observed only at low energies and are characterized by the same positions as the maxima related to the FCT-like Fe at 4.5 ML $\leqslant d \leqslant$ 10 ML. Thus, the $I(E)$ curve for the 4 ML film becomes exactly the same as that for the films with 4.5 ML $\leqslant d \leqslant$ 10 ML, which is also clearly seen from the direct comparison of the $I(E)$ curves for 4, 4.5, 5 and 7 ML film in Fig. 3b (also the difference from the curves for 2 and 3 ML is very pronounced). From this it follows that the 4 ML film

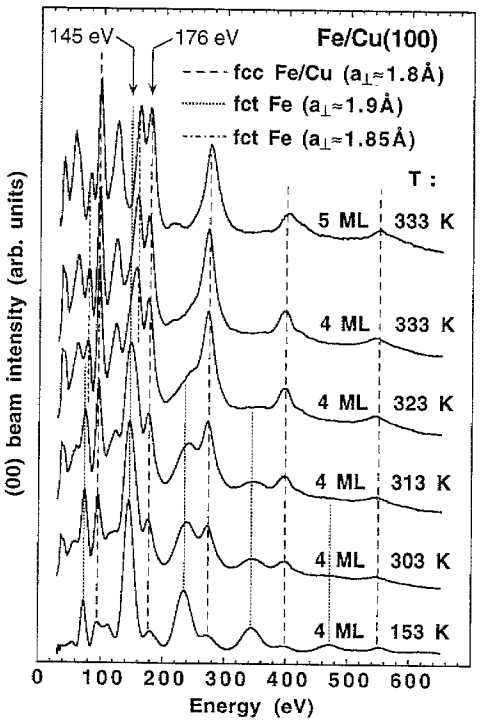

Fig. 7. Intensity versus energy dependence of the LEED (0 0) beam for 4 ML Fe on Cu(1 0 0) measured at various temperatures during heating. The kinematic maxima related to the FCC-like ($a_\perp \approx 1.8$ Å) and two different FCT-like ($a_\perp \approx 1.9$ and 1.85 Å) structures of Fe on Cu(1 0 0) are traced by vertical dashed, dotted and dashed-dotted lines, respectively. The $I(E)$ peaks associated with the FCC-like Fe overlaps with an analogous peaks for Cu(1 0 0). At low temperatures only the maxima related to the FCT-like Fe with $a_\perp \approx 1.9$ Å are observed. During heating these maxima disappear completely between 313 and 333 K, and the new $I(E)$ peaks associated with the FCT-like Fe with $a_\perp \approx 1.85$ Å appear.

at $T = 333$ K assumes a similar structure as the 5–9 ML films, namely an FCC-like structure in the bulk of the film and FCT-like in the topmost layers.

The values of $a_\perp$ derived from the Fig. 3b are presented in Fig. 4b. The structural transformation observed in the 4 ML film reveals itself in this figure too. Whereas the values of $a_\perp$ (FCT-like Fe) for the 2 and 3 ML film remain the same, this value changes abruptly for the 4 ML film and becomes approximately the same as the ones for 4.5 ML $\leqslant d \leqslant 10$ ML. Like in the low-temperature case (Fig. 3a) two different fixed values of $a_\perp$ are observed in different coverage regions; each of these values seems to decrease very little upon heating as compared to those in Fig. 3a (such a decrease was also observed previously in Ref. [4]).

3.3. Magnetic properties of Fe/Cu(1 0 0) as a function of thickness and temperature

Both the thickness and temperature dependences of the magnetic properties of Fe/Cu(1 0 0) obtained by us are consistent with the results of previous investigations [9, 17, 18]. We did not attempt to remeasure these dependencies very precisely (because this has been done before), but just intended to establish tendencies and critical points as well as to compare our data with literature values. The thickness dependence of the saturation magnetization extrapolated to $T = 0$ for the hysteresis loops measured using polar MOKE is presented in Fig. 8a. As observed previously, two regions with different magnetic properties can be distinguished over the thickness range where FCC/FCT-like Fe exists. Up to about 4 ML, the saturation magnetization increases linearly with film thickness which is related to the growth of a homogeneous ferromagnetic FCT-like Fe film. Slightly above 4 ML the saturation magnetization decreases sharply following the structural phase transformation of the ferromagnetic FCT-like Fe into paramagnetic (or antiferromagnetic at low temperature) FCC-like Fe; only the topmost Fe layers retain the FCT-like structure and remain ferromagnetic. At higher d the saturation magnetization is observed to be constant with increasing thickness (up to the FCC-BCC phase transition) indicating that the growing number of inner layers of the film (FCC-like Fe) does not contribute to the observed Kerr signal and the amount of the on-top ferromagnetic FCT-like Fe does not change significantly.

The main parameter characterizing the temperature dependence of the magnetic properties of a ferromagnetic system is the Curie temperature T_c; the thickness dependence of T_c obtained by extrapolating the temperature dependence of the saturation magnetization at fixed thicknesses to zero temperature is depicted in Fig. 8b. The reason

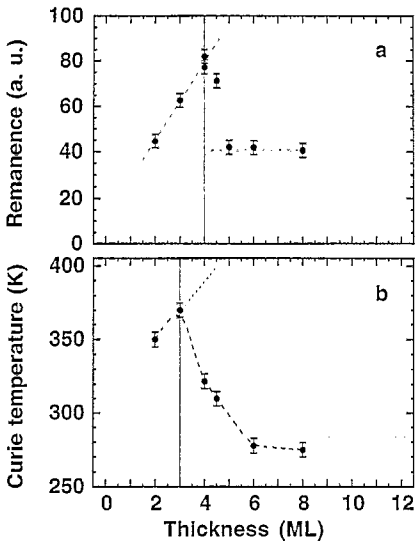

Fig. 8. (a) Thickness dependence of the saturation magnetization extrapolated to $T = 0$ for the hysteresis loops measured using magneto-optical Kerr effect as well as (b) the Curie temperatures obtained by extrapolating the temperature dependence of the saturation magnetization at a fixed thickness to 0 K. Both the character of $M(d)$ and $T_c(d)$ dependences as well as the values of T_c agree rather well with previous investigations [9, 17, 18]. Dashed lines serve as a guide to the eye. The dotted line in (b) extrapolates the $T_c(d)$ dependence from the range below 3 ML to higher thicknesses.

to use the saturation magnetization (instead of the remanent one as usual) for the determination of T_c is an inclined shape of the hysteresis loops in Fe/Cu(1 0 0) near the ferromagnetic–paramagnetic transition. Such a shape results in a reduction of the remanent magnetization at temperatures of 10–25 K below the transition while the saturation magnetization remains relatively large and decreases rather slowly with increasing temperature. The saturation magnetization was also used previously [17] to determine the thickness dependence of the Curie temperature in Fe/Cu(1 0 0).

In the case of systems with reduced dimensionality, like a thin ferromagnetic film, this dependence is governed by a scaling law [37]. This law states that T_c should increase with increasing film thicknesses as long as the whole film is magnetic and no other properties of the system (structure, morphology, composition) are changed. From the point of view of the scaling law the thickness dependence of the Curie temperature in Fig. 8b approximately agrees with the thickness dependence of the saturation magnetization except for one difference, namely, a distinct decrease of T_c between 3 and 4 ML. This unusual behavior was not discussed previously (except for our previous Letter [28]) and we provide evidence that indeed an important property of the system, namely, its structure, is altering already at 4 ML thickness by temperature variation. To relate the observed decrease of T_c to this structural transformation one needs to consider the temperature dependencies of the magnetic properties and of the structure in a 4 ML film, simultaneously.

For such an analysis one needs a parameter which can quantitatively characterize the structural transformations in the system. Because this transformation affects simultaneously the FCC- and FCT-like phases of Fe, a good choice for such a parameter is the intensity ratio for two corresponding (the same order of the Bragg diffraction) kinematic $I(E)$ peaks related to these phases. This ratio $I(\mathrm{FCT})/I(\mathrm{FCC})$ then reveals the relation between the FCT- and FCC-like phases in the Fe film. The most intense kinematic maxima are best suited to calculate such a ratio; therefore, the peaks at $\approx$145 and 176 eV related to the FCT-like and FCC-like Fe, respectively, were chosen. Thus, the ratio $I_{145}(\mathrm{FCT})/I_{176}(\mathrm{FCC})$ was calculated.

In Fig. 9 the ratio $I_{145}(\mathrm{FCT})/I_{176}(\mathrm{FCC})$ as well as the saturation magnetization M_{sat} are presented as a function of temperature. The latter was increased from 150 to 343 K and then decreased to 190 K by steps of 5–30 K. A comparison of these two plots shows that they are practically identical for increasing temperature; the same curve can be used (dashed line in Fig. 9a and Fig. 9b) to fit both experimental curves. If another pair of the kinematic $I(E)$ peaks is taken, the corresponding ratio behaves in the same way: it decreases slowly during heating to 313 K and then drops fast between 313 and 333 K. The coincidence between the temperature behavior of M_{sat} and the ratio $I(\mathrm{FCT})/I(\mathrm{FCC})$ (Fig. 9) indicates that the ferromagnetic long-range order in the 4 ML film is not destroyed in the usual

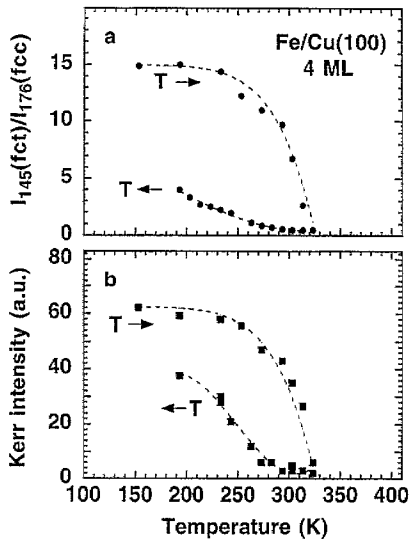

Fig. 9. Comparison of the temperature dependences of structural composition and magnetic properties for 4 ML Fe/Cu(1 0 0): the ratio of the intensity of the peaks at 145 and 176 eV (marked in Fig. 7) in the $I(E)$ curves for the (0 0) beam (a), as well as the saturation magnetization (b) during heating and cooling of the sample (indicated by arrows) through the order–disorder magnetic transition. The kinematic peaks at 145 and 176 eV are related to the FCT-like ($a_\perp \approx 1.9$ Å) and FCC-like Fe, respectively. Dashed lines serve as a guide to the eye. Identical dashed lines are used to trace the temperature dependence of both the ratio I_{145}/I_{176} in (a) and the saturation magnetization in (b) during heating.

thermodynamic way, but by the temperature-driven structural transformation. This phenomenon will be discussed in detail in the next section after a short analysis of the LEED results.

4. Discussion

We start our discussion with the $I(E)$ data in Fig. 3a. The analysis of the curves presented in this figure within the kinematic approximation provides essentially the same thickness dependence for the structure of the FCC-like Fe films at low temperature as previous LEED investigations [3, 5–8]: the whole film is vertically expanded at $d \leqslant 4$ ML whereas both the tetragonally expanded (in the topmost layers) and 'isotropic' FCC-like structures coexist at higher d before the FCC–BCC structural transformation sets in. The values of $a_\perp$ (Fig. 4a) evaluated from the $I(E)$ curves in Fig. 3a also agree rather well with the tensor LEED data, which assume $a_\perp = 1.78$ and 1.87 Å for the FCC- and FCT-like Fe, respectively, in the entire thickness region where FCC/FCT Fe exists. As compared to these values practically all our values of $a_\perp$ presented in Fig. 4a are shifted upwards by 0.01–0.03 Å. This systematic shift can be related to an inherent inaccuracy of the kinematic approximation as well as an incorrectness in the energy calibration of the LEED facility and/or charging effects in the LEED electrodes system.

There are two further differences between our data and the previous LEED results. First, at fixed d only one value of $a_\perp$ for the totally expanded film ($d \leqslant 4$ ML) follows from the $I(E)$ curves in Fig. 3a, whereas the tensor LEED analysis obtains a variation of $a_\perp$ within the film (a coexistence of pronouncedly different values of $a_\perp$ within the film should results either in a superposition of several periodic sequences or in a broadening of the observed kinematic maxima; neither such a superposition nor a broadening are discernible in our $I(E)$ curves at $d \leqslant 4$ ML). Second, the average values of $a_\perp$ for the expanded phase are approximately constant at $d \leqslant 4$ ML and 4.5 ML $\leqslant d < 10$ ML at fixed temperature, but differ from each other. This implies *different average tetragonal expansions* (≈ 1.9 and 1.85 Å) in the FCT-like Fe on Cu(1 0 0) for the entirely expanded FCC-like Fe film and the film expanded only in the topmost layers, whereas previous LEED investigations claim the same average values of $a_\perp$ (1.87 Å) for the FCT-like Fe over the whole thickness region where the FCC/FCT-like Fe exists. These investigations give the value of 1.90 Å for only one of the interlayer spacings in the 4 ML Fe film (the entirely FCT-like film); other layers, which are less expanded, should result in reducing the average tetragonal expansion to 1.87 Å. In our case, the change of the average vertical interlayer spacing for the FCT-like phase at $d > 4.5$ ML as compared to that at $d \leqslant 4$ (from ≈ 1.9 to 1.85 Å) cannot only be implied from the kinematic analysis of the presented $I(E)$ curves (Fig. 4a) but also directly traced from these curves (Fig. 3a) by following the energy position of the

maxima related to the FCT-like Fe. At $d = 4.5$ ML this change is not complete; the maxima associated with the FCT-like Fe still contain some contribution from the $I(E)$ peaks related to the FCT-like Fe with $a_\perp = 1.9$ Å. This contribution is, e.g., clearly seen as a shoulder at the left-hand side of the peak at 156 eV or as a broadening of the peak at 349 eV. As to the observed difference in the value of the average tetragonal expansion for the entirely expanded FCC-like Fe film and the film expanded only in the topmost layers, it cannot be related to some scattering processes stemming from the topmost location of the expanded layer in the 4.5–10 ML Fe films. The maxima associated with the FCT-like Fe in the $I(E)$ curve for the 2 ML film (which also represent an FCT-like structure of comparable thickness on top of an FCC lattice) have essentially the same energetic positions as analogous maxima for the 3 and 4 ML films. The modification of the superstructure can also be excluded as a reason for the observed difference; the $I(E)$ maxima related to the FCT-structure do not significantly vary their energetic positions in the range of thicknesses between 2 and 4 ML while an essential change of the superstructure occurs.

Apart from these two minor disagreements the general evolution of the structure of Fe/Cu(1 0 0) with increasing thickness obtained in the previous LEED investigations is exactly reproduced by us. This justifies the conclusion that the kinematic approximation can provide reliable results for this specific system. Energy positions of the kinematic maxima either for Cu, or FCC- or FCT-like Fe show very small deviations from the linear dependences as functions of n^2 (see Fig. 5) and the values of the inner potential given by the kinematic approximation ($V_0 = 12$–15 eV) are also rather reasonable.

The reasons why the kinematic approximation works so well in the case of Fe/Cu(1 0 0) (and the thin films of some other 3d-metals [13, 32–34]) are not completely clear. Generally, the kinematic (or single-scattering) approximation is well applicable in the case of a weak electron–atom scattering or in situations where the unit-cell dimensions of the periodic lattice are large compared to the mean free path of the electrons [30, 31]. In other words, it is a concurrence of the elastic and inelastic scattering that determines the suitability of the kinematic approach for each individual case. Because of the strong energy dependence of both the elastic and inelastic scattering, a balance between these two processes depends not only on the material but also on the kinetic energy. This can be clearly seen in Fig. 3: whereas some multiple-scattering maxima are observed at the kinetic energies below 200–250 eV, only the 'kinematic' peaks have a pronounced intensity at higher energies. It is exactly the occurrence of these peaks which allows the identification of the kinematic intensity maxima in the region where the multiple-scattering cannot be neglected.

The applicability of the kinematic approximation for investigating the thickness dependence of the structure of Fe/Cu(1 0 0) implies that the analysis of the $I(E)$ curves for the (0 0) beam within this approach should also provide reliable results for the temperature dependence of the structure of Fe/Cu(1 0 0). As it was noted in Section 3.2, two main tendencies are observed in the temperature dependence of the $I(E)$ curves: (i) the relative weight of the maxima related to the FCT-like Fe decreases with increasing temperature as compared to the $I(E)$ peaks for Cu ($d \leqslant 3$ ML) and FCC-like Fe (5 ML $\leqslant d \leqslant 10$ ML), and (ii) the diffraction peaks at higher kinetic energies are attenuated stronger than the peaks at lower kinetic energies.

The larger attenuation of the maxima related to the FCT-like Fe as compared to the $I(E)$ peaks from Cu and FCC-like Fe can be partly understood considering that FCT-like Fe is always located in the topmost layers of our sample: at $d \leqslant 4$ ML FCT-like Fe covers the substrate and at 5 ML $\leqslant d \leqslant 10$ ML (4 ML $\leqslant d \leqslant 10$ ML at $T \geqslant 333$ K) this structure is placed on top of the FCC-like Fe. Generally, the temperature-induced displacement of the atoms in the top layer of a single crystal can be larger by a factor of 2 than that in the deeper layers [30]. In the case of an evaporated layer, which is characterized by a rather extended surface and strong buckling [3–9], this effect can be even more pronounced, and thus, may lead to the observed change of the $I(E)$ curves.

As to the different attenuation of the $I(E)$ peaks at low and high kinetic energies, two phenomena which produce opposite effects should be considered. On the one hand, the influence of the

temperature on the $I(E)$ peaks increases with increasing energy, because the anti-Bragg phase differences introduced by a given (temperature-induced) displacement are greater at shorter wavelength (higher energies). On the other hand, the effective escape length is smaller at lower energies which will support a stronger attenuation of the corresponding $I(E)$ maxima with increasing temperature because of the enhanced displacement of atoms in the surface layers. Whereas in a single crystal these two contributions are approximately of the same order (at least not at very high kinetic energies), in ultrathin overlayers of several ML thicknesses the second contribution becomes of minor importance. The effective escape length is then essentially determined by the thickness of the overlayer and is practically the same for both low and high energies. The $I(E)$ peaks in these two energy regions will then be related to the temperature-induced atom displacement of the same order which will result in a stronger attenuation of the high-energy maxima with increasing temperature. This effect will be additionally amplified by the enlarged atom displacements in ultrathin overlayers which can lead to the observed large temperature-induced attenuation of the $I(E)$ maxima related to the FCT-like Fe at high energy.

This argument can also be reversed: the very strong attenuation of the $I(E)$ peaks at high energy with increasing temperature represents an indirect sign that the corresponding crystalline phase is placed in the topmost layers of the sample. Thus, we get additional evidence that the FCT-like Fe at 4–5 ML $\leqslant d \leqslant$ 10 ML is placed on the top of the FCC-like Fe.

Generally, all the considerations above explain, at least qualitatively, the observed tendencies in the temperature dependence of the $I(E)$ curves. Nevertheless, it cannot be completely excluded that some minor structural changes take place; dynamical LEED calculations are necessary to extract this information and to make some definitive conclusions.

Such conclusions, however, can be done in the cases of 4 and 4.5 ML films on the basis of the presented data due to the dramatic changes of the corresponding $I(E)$ curves at temperature variation. As it follows from Fig. 7, the $I(E)$ curve for the 4 ML film heated up to $\approx$333 K becomes exactly the same as that for the films with 4.5 ML $\leqslant d \leqslant$ 10 ML, which imply that the 4 ML film at $T \geqslant$ 333 K assumes a similar structure as the 5–9 ML films, namely, an FCC-like structure in the bulk of the film and FCT-like in the topmost layers. This structural transition is an explanation for the observed disagreement between the temperature dependence of the saturation magnetization and that of the Curie temperature mentioned in Section 3.3. As it was noted in this section, in the case of systems with reduced dimensionality, like a thin ferromagnetic film, the thickness dependence of the Curie temperature is governed by the scaling law [38]. This law requires T_c to increase with increasing film thickness as long as the whole film is magnetic and no other properties of the system (structure, morphology, composition) are changed. If these conditions were fulfilled in Fe/Cu(1 0 0), one would expect an increase of T_c with increasing film thickness up to 4 ML, a distinct decrease slightly above this thickness and some constancy at larger d. What was observed instead by us (Fig. 8b) and previously by Thomassen et al. [17] is a monotonous increase of T_c with film thickness up to about 3 ML (a maximum of T_c at $d \approx 3$ ML was observed also in Ref. [39]) and a distinct decrease of T_c at 4 ML. This is difficult to understand, because the structural phase transformation from the entirely FCC-like structure with a tetragonal expansion to that expanded only in the topmost layers was thought to occur at higher thicknesses. This is also to be expected from the behavior of the saturation magnetization extrapolated to 0 K (Fig. 8a). Our analysis of the temperature dependence of the $I(E)$ curves provides evidence that indeed an important property of the system, namely, its structure, is altering already at 4 ML thickness by temperature variation.

Additionally, the coincidence between the temperature behavior of M_{sat} and the ratio I(FCT)/I(FCC) (Fig. 9) indicates that the ferromagnetic long-range order in the 4 ML film is not destroyed in the usual thermodynamic way, but by the temperature-driven structural transformation. An observed irreversibility of the ferromagnetic–paramagnetic transition (Fig. 9) also supports this conclusion, pointing towards an activated process.

For the thicker Fe films ($d > 4.5$ ML) the restriction of the FCT-like structure only to the topmost layers is energetically more favorable, than an overall FCT-like structure. The corresponding reduction of the elastic energy in the film should then overcompensate the increase of the interfacial energy. Additionally, some energy barrier between two different structural states can exist and must then be overcome. At a fixed thickness, the temperature affects both the balance between elastic and interfacial energies and the probability to overcome the effective barrier. If such a barrier really exists and the depth of the potential minima on its opposite sides is different, a temperature irreversibility of the structural transition can be expected. Such an irreversibility is in fact observed in Fig. 9a: the 4 ML film turns into the new structural state after heating and keeps this new structure even during subsequent cooling. The onset of the ferromagnetic long-range order occurs then at $T \approx 270$–280 K (Fig. 9b), which is the typical Curie temperature for the Fe film with FCC-like structure expanded only in the topmost layers (see Fig. 8). The initial FCT-like structure with $a_\perp \approx 1.9$ Å ($a_\perp$ for the FCT-like structure changes to 1.85 Å after the structural transition) appears in the same temperature range (Fig. 9a); two different FCT-like structures ($a_\perp \approx$ 1.85 and 1.9 Å) and the FCC-like structure coexist in a rather extended range of temperatures. Only after cooling down to temperatures T_{min} of about 120–180 K the system slowly returns to the initial structural state and to the full magnetization. The time scale of this process depends on the cooling procedure and T_{min} and varies from 20 to 30 min to some hours.

The appearance of the ferromagnetic FCT-Fe with $a_\perp \approx 1.85$ Å (placed on the top of the Fe film) explains some disagreement between temperature dependences of M_{sat} and the ratio $I_{145}(FCT)/I_{176}(FCC)$ observed during cooling (Fig. 9). The point is that the value of M_{sat} represents the joint saturation magnetization of both ferromagnetic phases in the system ($a_\perp \approx 1.85$ and 1.9 Å) whereas only the FCT-Fe with $a_\perp \approx 1.9$ Å is taken into account by the ratio $I_{145}(FCT)/I_{176}(FCC)$. During heating the FCT-Fe with $a_\perp \approx 1.85$ Å appears only at temperatures above 310 K which significantly exceed the value of T_c (≈ 270 K) for this specific structure. The latter does not contribute therefore to M_{sat} which means that during heating both the saturation magnetization and the ratio $I_{145}(FCT)/I_{176}(FCC)$ are exclusively related to the FCT-Fe with $a_\perp \approx 1.9$ Å. The whole situation changes, however, during cooling because the FCT-Fe with $a_\perp \approx 1.85$ Å does not disappear at $T \approx 310$ K but exists in a rather extended range of temperatures. As soon as the temperature decreases below ≈ 270 K, the FCT-Fe with $a_\perp \approx 1.85$ Å becomes ferromagnetic and begin to contribute to M_{sat}. This is, in fact, observed in Fig. 9 as a strong increase of the saturation magnetization at $T \approx 270$ K during cooling. At the same time the value of $I_{145}(FCT)/I_{176}(FCC)$ is relatively small because of a small portion of the FCT-Fe with $a_\perp \approx 1.9$ Å. This portion increases with the further decrease of the temperature (the portion of the FCT-Fe with $a_\perp \approx 1.85$ Å decreases at the same time) which results in the reestablishment of the relation between M_{sat} and the ratio $I_{145}(FCT)/I_{176}(FCC)$.

The maximum temperature to which the 4 ML film was heated (343 K) is significantly lower than that for the onset of interdiffusion (410 K [15, 36]). Nevertheless, if some influence of this process on the structure would take place at lower temperatures [37], it should reveal itself in the same way not only in the 4 ML film but also in the 3 ML film, where the onset of interdiffusion occurs at even lower temperature [15, 36, 37]. The dependences of M_{sat} and $I_{145}(FCT)/I_{176}(FCC)$ on T for the 3 ML film are depicted in Fig. 10a and Fig. 10b, respectively, the same scaling as in Fig. 9 being used. The ratio $I(FCT)/I(FCC)$ in Fig. 9a decreases slowly with increasing temperature, but has in no way the same behavior as M_{sat} and shows no abrupt changes between 313 and 333 K (as it occurs in the 4 ML film) or in the region of the Curie transition at ≈ 365 K. If the structure of the 3 ML film is, however, to some extent affected by the temperature, the corresponding changes are not as dramatic as in the 4 ML film and do not significantly influence the magnetic properties. The reversibility of both dependences in Fig. 10a and Fig. 10b supports this conclusion. The observed structural and magnetic transitions are in fact characteristic for the 4 ML film, which seems to be structurally unstable because of the competition of the elastic and

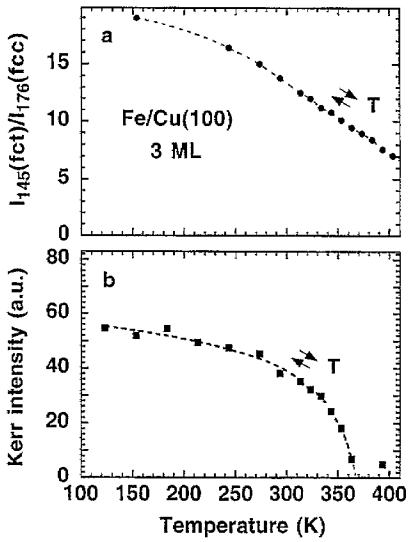

Fig. 10. Comparison of the temperature dependences of structural composition and magnetic properties for 3 ML Fe/Cu(1 0 0): the ratio of the intensity of the peaks at 145 and 176 eV in the $I(E)$ curves for the (0 0) beam (a), as well as saturation magnetization (b) during heating and cooling of the sample (indicated by arrows) through the Curie transition. The kinematic peaks at 145 and 176 eV are related to the FCT-like ($a_{\perp} \approx 1.9$ Å) and FCC-like Fe, respectively. Dashed lines represent a guide to the eye. The same scales as in Fig. 9a and Fig. 9b are used in (a) and (b), respectively.

interfacial energies. Just increasing the thickness by 0.5 ML or heating up to 333 K is sufficient to force the film into the new structural and magnetic state.

Thus, the strange behavior of the thickness dependence of the Curie temperature T_c in Fe/Cu(0 0 1) discussed above can now be explained. By extrapolating the $T_c(d)$ dependence in Fe/Cu(1 0 0) from the range below 3 ML to $d = 4$ ML, the thermodynamical Curie temperature of the 4 ML film can be estimated to be approximately 390–400 K. But before the regular Curie transition can occur, a structural rearrangement takes place. The new structure which the 4 ML film assumes at $T \geqslant 333$ K also possesses ferromagnetic properties, but the corresponding Curie temperature (≈ 270 K) is significantly lower than 333 K. As soon as the structural transformation takes place, the film happens to be above T_c for this particular system and consequently becomes paramagnetic.

The 4.5 ML film also undergoes temperature-driven structural transformations affecting magnetic properties of this film. Whereas two different FCT-like structures of Fe ($a_{\perp} \approx 1.85$ and 1.9 Å) coexist at $T = 153$ K (together with the FCC-like Fe), only the FCT-like structure with the smaller tetragonal distortion ($a_{\perp} \approx 1.85$ Å) remains after heating up to 323 K. The latter is located exclusively in the topmost layers of the film and is characterized by the value of $T_c \approx 270$ K. The FCT-like structure with the larger tetragonal distortion ($a_{\perp} \approx 1.9$ Å) which we associate with the 'bulk' ferromagnetism in Fe/Cu(1 0 0) disappears completely in the temperature range between 293 and 313 K (Fig. 6). Considering that the value of T_c in 4.5 ML film is equal to ≈ 312 K (Fig. 8) one may reasonably assume that a magnetic order–disorder transition in this case is also mediated by the temperature-driven structural transformations. This phenomenon is completely analogous to the case of 4 ML (discussed in detail before) except for the different phase composition of the film at low temperature.

The fact that two different FCT-like structures exist in Fe/Cu(1 0 0) should be addressed in more detail. Both phases are characterized by an enlarged atomic volume and possess ferromagnetic properties. The most interesting question which arises, is whether the magnetic moments of these two phases are different, because the first-principle calculations for FCC-Fe [1, 2, 40] give not one but two ferromagnetic solutions with different values of the magnetic moment, namely, the so-called high-spin and low-spin phases, which exclusively exist at an enlarged atomic volume. This question seems to be answered negatively by the recent nonlinear magneto-optical Kerr effect (MOKE) investigations [22] claiming a constancy in the surface magnetization (and consequently, in the magnetic moment) in the entirely FCT-like Fe film and in the film expanded only in the topmost layers. These are the structures where we observe a difference in the tetragonal expansion of FCT-like Fe. This means that the magnetic moment of the tetragonally expanded FCC-like Fe/Cu(1 0 0) has to be rather insensitive to the value of the tetragonal expansion.

Taking into consideration the magnetic-phase diagram [1, 2] which implies an existence of the high-spin solution in a more or less extended range of the atomic volume, whereas this range is rather limited in the case of the low-spin solution, we can claim that the ferromagnetic FCT-like Fe/Cu(1 0 0) seems to exist as the high-spin phase. This conclusion is at variance with inverse photoemission results for ferromagnetic Fe/Cu(1 0 0) [41] but in agreement with the most recent MOKE and spin-resolved photoemission investigations of this system [42, 43].

5. Conclusions

We have shown that the structure of FCC-like Fe films grown at room temperature on Cu(1 0 0) changes not only as a function of coverage, as was found before, but also as a function of temperature. This phenomenon is observed in the 4 and 4.5 ML Fe films whose structures are extremely unstable because of the delicate balance between elastic and interfacial energies. As the parameter which predominantly determines the magnetic properties of FCC-like Fe, namely, the atomic volume, is affected by the structural transformation, such changes have a direct impact on magnetic properties of this system. When these structural transformations encompass the whole film, the ferromagnetic long-range order breaks down completely and the system becomes paramagnetic. Thus, a new kind of magnetic order–disorder transition, namely, a temperature-driven structural rearrangement in thin epitaxial Fe films on Cu(1 0 0), affecting the existence of ferromagnetism in the films is observed. This phenomenon differs fundamentally from the regular thermodynamical Curie transition, which occurs when thermal fluctuations of the spins overcompensate their aligning interaction.

On the contrary, the observed magnetic order–disorder transition mediated by a temperature-driven structural transformation supports a close relationship between structural and magnetic properties of thin films and, in particular, of Fe/Cu(1 0 0), in complete agreement with first-principle calculations and previous experimental investigations. We believe that the question whether the ferromagnetism drives the structural reconstruction (from FCC- to FCT-like structure) or if the reconstruction with its increase of the atomic volume yields the ferromagnetism [8], can now be answered. The strong reduction of the Curie temperature in the 4 ML film because of the temperature-driven FCT–FCC structural transformation implies a predominant role of the structure in the interplay between structure and magnetism observed in Fe/Cu(1 0 0). Nevertheless some minor influence of the ferromagnetic long-range order on the film structure cannot be completely excluded.

Additionally, our results indicate a difference in the value of the average tetragonal expansion for the entirely expanded FCC-like Fe film and the film expanded only in the topmost layers, exclusively the spacing between the topmost and the topmost but one layer seems to be affected by the expansion in the latter case. The same change of the tetragonal expansion is observed both if the structural transition from the entirely FCT-like Fe film to the FCC/FCT-like Fe film happens as a result of increasing thickness (from 4 to 5 ML), and if this transition is driven by increasing temperature (4 and 4.5 ML).

The very simple structural analysis presented in this paper seems to give reliable results for FCC Fe/Cu(1 0 0). We could distinguish between all structural phases in this system as well as exactly reproduce the development of the structure with film thickness observed previously by detailed LEED investigations except for the difference in the average tetragonal expansions for the entirely expanded FCC-like Fe film and the film expanded only in the topmost layers. This disagreement was addressed in detail in Section 4. We just want to note once more that the different average tetragonal expansions in the FCT-like and FCC/FCT-like Fe films cannot only be implied from the kinematic analysis of the presented $I(E)$ curves but also directly traced from these curves as a pronounced difference in the energy positions of the maxima associated with FCT-like Fe in the entirely and partly expanded films, these maxima being well separated from both the structure related to the substrate (the entirely expanded FCC-like Fe film) and the structure associated with the FCC-like Fe (the film expanded only in the topmost layers).

Acknowledgements

We would like to thank Prof. K. Heinz, Prof. F. Jona and Prof. W. Moritz for discussions and B. Zada for technical assistance. M.Z. thanks the Max-Planck-Gesellschaft for a stipend. This work has been supported by BMBF under Grant No. 05 621 EFA and the DPG under Grant No. Schn. 353/3.

References

[1] V.L. Moruzzi, P.M. Marcus, K. Schwartz, P. Mohn, Phys. Rev. B 34 (1986) 1784.
[2] V.L. Moruzzi, P.M. Marcus, J. Kübler, Phys. Rev. B 39 (1989) 6957.
[3] K. Heinz, P. Bayer, S. Müller, Surf. Rev. Lett. 2 (1995) 89.
[4] M. Wuttig, J. Thomassen, Surf. Sci. 282 (1993) 237.
[5] P. Bayer, S. Müller, P. Schmeizl, K. Heinz, Phys. Rev. B 48 (1993) 17611.
[6] S. Müller, P. Bayer, A. Kinne, P. Schmeizl, K. Heinz, Surf. Sci. 322 (1995) 21.
[7] S. Müller, P. Bayer, A. Kinne, C. Reischl, R. Metzler, K. Heinz, Surf. Sci. 321–323 (1995) 723.
[8] K. Heinz, S. Müller, P. Bayer, Surf. Sci. 337 (1995) 215.
[9] S. Müller, P. Bayer, C. Reischl, K. Heinz, B. Feldmann, H. Zillgen, M. Wuttig, Phys. Rev. Lett. 74 (1995) 765.
[10] J. Giergiel, J. Shen, J. Woltersdorf, A. Kirilyuk, J. Kirschner, Phys. Rev. B 52 (1995) 8528.
[11] H. Magnan, D. Chandesris, B. Vilette, O. Heckmann, J. Lecante, Phys. Rev. Lett. 67 (1991) 859.
[12] A. Kirilyuk, J. Giergiel, J. Shen, J. Kirschner, Phys. Rev. B 52 (1995) R11672.
[13] A. Kirilyuk, J. Giergiel, J. Shen, M. Straub, J. Kirschner, Phys. Rev. B 54 (1996) 1050.
[14] M. Wuttig, B. Feldmann, J. Thomassen, F. May, H. Zillgen, A. Brodde, H. Hannemann, H. Neddermeyer, Surf. Sci. 291 (1993) 14.
[15] N. Memmel, Th. Detzel, Surf. Sci. 307–309 (1994) 490.
[16] P. Schmeizl, K. Schmidt, P. Bayer, R. Döll, K. Heinz, Surf. Sci. 312 (1994) 73.
[17] J. Thomassen, F. May, B. Feldmann, M. Wuttig, H. Ibach, Phys. Rev. Lett. 69 (1992) 3831.
[18] D. Li, M. Freitag, J. Pearson, Z.Q. Qiu, S.D. Bader, Phys. Rev. Lett. 72 (1994) 3112.
[19] J. Giergiel, J. Kirschner, J. Landgraf, J. Shen, J. Woltersdorf, Surf. Sci. 310 (1994) 1.
[20] M.T. Lin, J. Shen, J. Giergiel, W. Kuch, H. Jenniches, M. Klaua, C.M. Schneider, J. Kirschner, Thin Solid Films 275 (1996) 99.
[21] P.J. Rous, J.B. Pendry, D.K. Saldin, K. Heinz, K. Müller, N. Bickel, Phys. Rev. Lett. 57 (1986) 2951.
[22] M. Straub, R. Vollmer, J. Kirschner, Phys. Rev. Lett. 77 (1996) 743.
[23] R.D. Ellerbrock, A. Fuest, A. Schatz, W. Keune, R.A. Brand, Phys. Rev. Lett. 74 (1995) 3053.
[24] D.J. Keavney, D.F. Storm, J.W. Freeland, I.L. Grigorov, J.C. Walker, Phys. Rev. Lett. 74 (1975) 4531.
[25] W. Keune, A. Schatz, R.D. Ellenbrock, A. Fuest, K. Wilmers, R.A. Brand, J. Appl. Phys., in press.
[26] D.P. Pappas, K.-P. Kämper, H. Hopster, Phys. Rev. Lett. 64 (1990) 3179.
[27] D.P. Pappas, C.R. Brundle, H. Hopster, Phys. Rev. B 45 (1992) 8169.
[28] M. Zharnikov, A. Dittschar, W. Kuch, C.M. Schneider, J. Kirschner, Phys. Rev. Lett. 76 (1996) 4620.
[29] F. Baudelet, M.-T. Lin, W. Kuch, K. Meinel, B. Choi, C.M. Schneider, J. Kirschner, Phys. Rev. B 51 (1995) 12563.
[30] J.B. Pendry, Low Energy Electron Diffraction, Academic Press, London, 1974.
[31] L.J. Clarke, Surface Crystallography, Wiley, New York, 1985.
[32] R. Rochow, C. Carbone, Th. Dodt, F.P. Johnen, E. Kisker, Phys. Rev. B 41 (1990) 3426.
[33] M. Zharnikov, A. Dittschar, W. Kuch, K. Meinel, C.M. Schneider, J. Kirschner, Thin Solid Films 275 (1996) 262.
[34] W. Kuch, A. Dittschar, K. Meinel, M. Zharnikov, C.M. Schneider, J. Kirschner, Phys. Rev. B 53 (1996) 11621.
[35] J. Giergiel, H. Hopster, J.M. Lawrence, J.C. Hemminger, J. Kirschner, Rev. Sci. Instrum. 66 (1995) 3475.
[36] H. Zilligen, B. Feldmann, M. Wuttig, Surf. Sci. 321 (1994) 32.
[37] J. Shen, J. Giergiel, A.K. Schmid, J. Kirschner, Surf. Sci. 328 (1995) 32.
[38] G.A.T. Allan, Phys. Rev. B 13 (1970) 52.
[39] M. Stampanoni, Appl. Phys. A 49 (1989) 449.
[40] M. Podgorny, J. Magn. Magn. Mater. 78 (1989) 352.
[41] G.J. Mankey, R.F. Willis, F.J. Himpsel, Phys. Rev. B 48 (1993) 10284.
[42] D.E. Fowler, J.V. Barth, Phys. Rev. B 53 (1996) 5563.
[43] M. Zharnikov, A. Dittschar, W. Kuch, C.M. Schneider, J. Kirschner, J. Magn. Magn. Mater. 165 (1997) 250.